Multi-scale and angular analysis of ray-optical light trapping schemes in thin-film solar cells: Micro lens array, V-shaped configuration, and double parabolic trapper

Changsoon Cho and Jung-Yong Lee*

Graduate School of Energy, Environment, Water, and Sustainability (EEWS), Graphene Research Center, Korea Advanced Institute of Science and Technology (KAIST), Daejeon 305-701, South Korea
jungyong.lee@kaist.ac.kr

Abstract: An efficient light trapping scheme is a key to enhancing the power conversion efficiency (PCE) of thin-film photovoltaic (PV) cells by compensating for the insufficient light absorption. To handle optical components from nano-scale to micro-scale seamlessly, a multi-scale optical simulation is carefully designed in this study and is used to qualitatively analyze the light trapping performances of a micro lens array (MLA), a V-shaped configuration, and the newly proposed scheme, which is termed a double parabolic trapper (DPT) according to both daily and annual movement of the sun. DPT has the potential to enhance the PCE significantly, from 5.9% to 8.9%, for PCDTBT:$PC_{70}BM$-based polymer solar cells by perfectly trapping the incident light between two parabolic PV cells.

©2013 Optical Society of America

OCIS codes: (310.6845) Thin film devices and applications; (040.5350) Photovoltaic; (350.6050) Solar energy; (160.4890) Organic materials.

References and links

1. A. Goetzberger, "Optical confinement in thin Si-solar cells by diffuse back reflectors," in *Fifteenth IEEE Photovoltaic Specialists Conference*, pp. 867–870 (1981).
2. E. Yablonovitch, "Statistical ray optics," J. Opt. Soc. Am. A **72**(7), 899–907 (1982).
3. P. Campbell and M. A. Green, "Light trapping properties of pyramidally textured surfaces," J. Appl. Phys. **62**(1), 243–249 (1987).
4. M. A. Green, "Lambertian light trapping in textured solar cells and light-emitting diodes: Analytical solutions," Prog. Photovolt. Res. Appl. **10**(4), 235–241 (2002).
5. W. L. Bai, Q. Q. Gan, F. Bartoli, J. Zhang, L. K. Cai, Y. D. Huang, and G. F. Song, "Design of plasmonic back structures for efficiency enhancement of thin-film amorphous Si solar cells," Opt. Lett. **34**(23), 3725–3727 (2009).
6. R. Dewan, M. Marinkovic, R. Noriega, S. Phadke, A. Salleo, and D. Knipp, "Light trapping in thin-film silicon solar cells with submicron surface texture," Opt. Express **17**(25), 23058–23065 (2009).
7. O. Kluth, B. Rech, L. Houben, S. Wieder, G. Schope, C. Beneking, H. Wagner, A. Loffl, and H. W. Schock, "Texture etched ZnO: Al coated glass substrates for silicon based thin film solar cells," Thin Solid Films **351**(1-2), 247–253 (1999).
8. J. Krc, M. Zeman, O. Kluth, E. Smole, and M. Topic, "Effect of surface roughness of ZnO: Al films on light scattering in hydrogenated amorphous silicon solar cells," Thin Solid Films **426**(1-2), 296–304 (2003).
9. J. M. Lee, S. J. Yun, J. K. Kim, and J. W. Lim, "Texturing of Ga-Doped ZnO Transparent Electrode for a-Si: H Thin Film Solar Cells," Electrochem. Solid State **14**(11), B124–B126 (2011).
10. J. Muller, G. Schope, O. Kluth, B. Rech, V. Sittinger, B. Szyszka, R. Geyer, P. Lechner, H. Schade, M. Ruske, G. Dittmar, and H. P. Bochem, "State-of-the-art mid-frequency sputtered ZnO films for thin film silicon solar cells and modules," Thin Solid Films **442**(1-2), 158–162 (2003).
11. J. Muller, B. Rech, J. Springer, and M. Vanecek, "TCO and light trapping in silicon thin film solar cells," Sol. Energy **77**(6), 917–930 (2004).
12. B. Rech and H. Wagner, "Potential of amorphous silicon for solar cells," Appl. Phys. A-Mater. **69**, 155–167 (1999).
13. F. Ruske, C. Jacobs, V. Sittinger, B. Szyszka, and W. Werner, "Large area ZnO: Al films with tailored-light scattering properties for photovoltaic applications," Thin Solid Films **515**(24), 8695–8698 (2007).

#182307 - $15.00 USD Received 21 Dec 2012; revised 7 Feb 2013; accepted 9 Feb 2013; published 21 Feb 2013

14. J. Springer, B. Rech, W. Reetz, J. Muller, and M. Vanecek, "Light trapping and optical losses in microcrystalline silicon pin solar cells deposited on surface-textured glass/ZnO substrates," Sol. Energy Mater. Sol. Cells **85**, 1–11 (2005).
15. A. Abass, H. H. Shen, P. Bienstman, and B. Maes, "Angle insensitive enhancement of organic solar cells using metallic gratings," J. Appl. Phys. **109**(2), 023111 (2011).
16. C. J. Min, J. Li, G. Veronis, J. Y. Lee, S. H. Fan, and P. Peumans, "Enhancement of optical absorption in thin-film organic solar cells through the excitation of plasmonic modes in metallic gratings," Appl. Phys. Lett. **96**(13), 133302 (2010).
17. S. I. Na, S. S. Kim, J. Jo, S. H. Oh, J. Kim, and D. Y. Kim, "Efficient Polymer Solar Cells with Surface Relief Gratings Fabricated by Simple Soft Lithography," Adv. Funct. Mater. **18**(24), 3956–3963 (2008).
18. S. I. Na, S.-S. Kim, S. S. Kwon, J. Jang, K. Juhwan, T. Lee, and K. Dong-Yu, "Surface relief gratings on poly(3-hexylthiophene) and fullerene blends for efficient organic solar cells," Appl. Phys. Lett. **91**(17), 173509 (2007).
19. H. H. Shen and B. Maes, "Combined plasmonic gratings in organic solar cells," Opt. Express **19**(S6 Suppl 6), A1202–A1210 (2011).
20. K. Tvingstedt, N. K. Persson, O. Inganas, A. Rahachou, and I. V. Zozoulenko, "Surface plasmon increase absorption in polymer photovoltaic cells," Appl. Phys. Lett. **91**(11), 113514 (2007).
21. Z. F. Yu, A. Raman, and S. H. Fan, "Fundamental limit of light trapping in grating structures," Opt. Express **18**(S3 Suppl 3), A366–A380 (2010).
22. J. Y. Lee and P. Peumans, "The origin of enhanced optical absorption in solar cells with metal nanoparticles embedded in the active layer," Opt. Express **18**(10), 10078–10087 (2010).
23. K. Tvingstedt, S. Dal Zilio, O. Inganäs, and M. Tormen, "Trapping light with micro lenses in thin film organic photovoltaic cells," Opt. Express **16**(26), 21608–21615 (2008).
24. P. Peumans, V. Bulovic, and S. R. Forrest, "Efficient photon harvesting at high optical intensities in ultrathin organic double-heterostructure photovoltaic diodes," Appl. Phys. Lett. **76**(19), 2650–2652 (2000).
25. K. Tvingstedt, V. Andersson, F. Zhang, and O. Inganas, "Folded reflective tandem polymer solar cell doubles efficiency," Appl. Phys. Lett. **91**(12), 123514 (2007).
26. S. B. Rim, S. Zhao, S. R. Scully, M. D. McGehee, and P. Peumans, "An effective light trapping configuration for thin-film solar cells," Appl. Phys. Lett. **91**(24), 243501 (2007).
27. M. Niggemann, M. Glatthaar, P. Lewer, C. Muller, J. Wagner, and A. Gombert, "Functional microprism substrate for organic solar cells," Thin Solid Films **511**, 628–633 (2006).
28. P. Peumans, A. Yakimov, and S. R. Forrest, "Small molecular weight organic thin-film photodetectors and solar cells," J. Appl. Phys. **93**(7), 3693–3723 (2003).
29. L. A. A. Pettersson, L. S. Roman, and O. Inganas, "Modeling photocurrent action spectra of photovoltaic devices based on organic thin films," J. Appl. Phys. **86**(1), 487–496 (1999).
30. S. H. Park, A. Roy, S. Beaupre, S. Cho, N. Coates, J. S. Moon, D. Moses, M. Leclerc, K. Lee, and A. J. Heeger, "Bulk heterojunction solar cells with internal quantum efficiency approaching 100%," Nat. Photonics **3**(5), 297–302 (2009).
31. J. Jin, J. Lee, S. Jeong, S. Yang, J.-H. Ko, H.-G. Im, S.W. Baek, J.Y. Lee, and B.S. Bae, "High-performance hybrid plastic films: A robust electrode platform for thin-film optoelectronics," Energy Environ. Sci., DOI: 10.1039/c3ee24306k
32. X. H. Li, W. C. H. Choy, L. J. Huo, F. X. Xie, W. E. I. Sha, B. F. Ding, X. Guo, Y. F. Li, J. H. Hou, J. B. You, and Y. Yang, "Dual plasmonic nanostructures for high performance inverted organic solar cells," Adv. Mater. (Deerfield Beach Fla.) **24**(22), 3046–3052 (2012).
33. T. K. Mallick and P. C. Eames, "Design and fabrication of low concentrating second generation PRIDE concentrator," Sol. Energy Mater. Sol. Cells **91**(7), 597–608 (2007).
34. K. Yoshioka, K. Endoh, M. Kobayashi, A. Suzuki, and T. Saitoh, "Design and properties of a refractive static concentrator module," Sol. Energy Mater. Sol. Cells **34**(1-4), 125–131 (1994).
35. K. Yoshioka, A. Suzuki, and T. Saitoh, "Performance evaluation of two-dimensional compound elliptic lens concentrators using a yearly distributed insolation model," Sol. Energy Mater. Sol. Cells **57**(1), 9–19 (1999).
36. S. Dal Zilio, K. Tvingstedt, O. Inganas, and M. Tormen, "Fabrication of a light trapping system for organic solar cells," Microelectron. Eng. **86**(4-6), 1150–1154 (2009).

1. Introduction

As global energy and environment problems become important issues, the demand for solar energy as an alternative energy source has greatly increased. Crystalline silicon (c-Si) bulk photovoltaic (PV) cells are the most popular types of cells in the commercial solar cell market due to their high power conversion efficiency (PCE) of approximately 20%, but the cost of power generation with these cells is still high compared to that of fossil fuels. On the other hand, thin-film PVs using materials such as amorphous silicon and organic materials have been recently considered as alternatives for bulk PVs to reduce the price by curtailing the material cost. In addition to their low cost, their thin-film characteristics allow the creation of light, colorful and flexible solar cells systems. However, their thin active layers are a major drawback to their commercialization due to the low light absorption of these layers. Because a high proportion of the incident light energy is not absorbed in the active layer and is merely

#182307 - $15.00 USD Received 21 Dec 2012; revised 7 Feb 2013; accepted 9 Feb 2013; published 21 Feb 2013
(C) 2013 OSA

reflected out, the full potential in terms of the PCE has yet to be achieved. Therefore, proper light trapping schemes to increase the optical path length of the incident light in the active layer should be studied in an effort to overcome the drawbacks of thin-film PVs and increase the PCE.

For bulk solar cells, it is known that surface texturing on the active layers at a scale tens of micrometers can increase the optical path length to $4n^2$ compared to the active layers thickness in which n is the refractive index of the active material [1–4]. Because the active layers of the bulk solar cells are sufficiently thick to be incoherent, the light trapping effect follows the ray-optical regime. The usual structures of thin-film solar cells, on the other hand, can be separated into two parts: an incoherent glass substrate and a coherent multilayer region containing the active layer. Hence, both the ray-optics and the wave-optics should be taken into account in thin-film solar cells. Previously proposed light trapping schemes using wave-optical regimes mostly include interface texturing between the thin-film layers [5–14] or the surface plasmon polariton (SPP) effect to concentrate the field intensity within the active layer [15–22]. Compared to these wave-optical schemes, ray-optical light trapping regimes that modify the incoherent region have some advantages, as they can avoid the electrical defect which can arise in the wave-optical regime by modifying the active layer, while the absorption enhancement characteristic works for a broadband spectrum rather than a specific narrowband spectrum. Such ray-optical schemes have recently been studied [23–27], but theoretical analyses of these schemes are relatively rare.

To devise optimal ray-optical light trapping schemes, their performances should be precisely appraised by a proper simulation analysis and should be fairly compared to those of other schemes. However, thin-film PVs have both coherent regions consisting of a nanometer-scale multilayer structure and incoherent regions consisting of micrometer-scale optical components such as a substrate. For this reason, it is not a simple matter to evaluate the spectral response of these devices without proper analytical schemes. Therefore, a multi-scale approach is necessary for an accurate estimation of the light trapping performances of different configurations in thin-film PVs. Moreover, because most light trapping schemes are influenced by the incident angle and given that a solar-tracking system is generally not feasible for use in thin-film PVs at a low cost, the optical property only at the normal incident angle does not sufficiently represent the performance of the PV system. A simulation study should take the entire range of incident angle variation as caused by the annual sun movement into consideration, though this has been often neglected.

Here, we implement an optical simulation to consider both ray-optical and wave-optical characteristics and use it for a precise evaluation of the angular performances of previously proposed light trapping schemes, a micro lens array (MLA) and V-shaped configurations. Moreover, we propose an ideal configuration, which we term double parabolic trapper (DPT) using the geometrical characteristics of the parabolas to achieve the theoretically perfect absorption of the incident light.

2. Multi-scale properties of thin-film PVs

The multi-scalability of thin-film PVs necessitates careful attention when conducting optical analyses, contrary to bulk PVs. In bulk cells with micro-scale active layers, incoherent ray-optics is sufficient to evaluate the optical performance. As a general rule, an oblique propagation angle is always considered to be advantageous to increase the optical path length in the bulk active layers. However, in thin-film PVs, both nano-scale and micro-scale structures coexist in the devices. As many nano-scale layers with different materials are stacked on the micro-scale substrate, geometrical path length enhancement by means of

#182307 - $15.00 USD Received 21 Dec 2012; revised 7 Feb 2013; accepted 9 Feb 2013; published 21 Feb 2013
(C) 2013 OSA

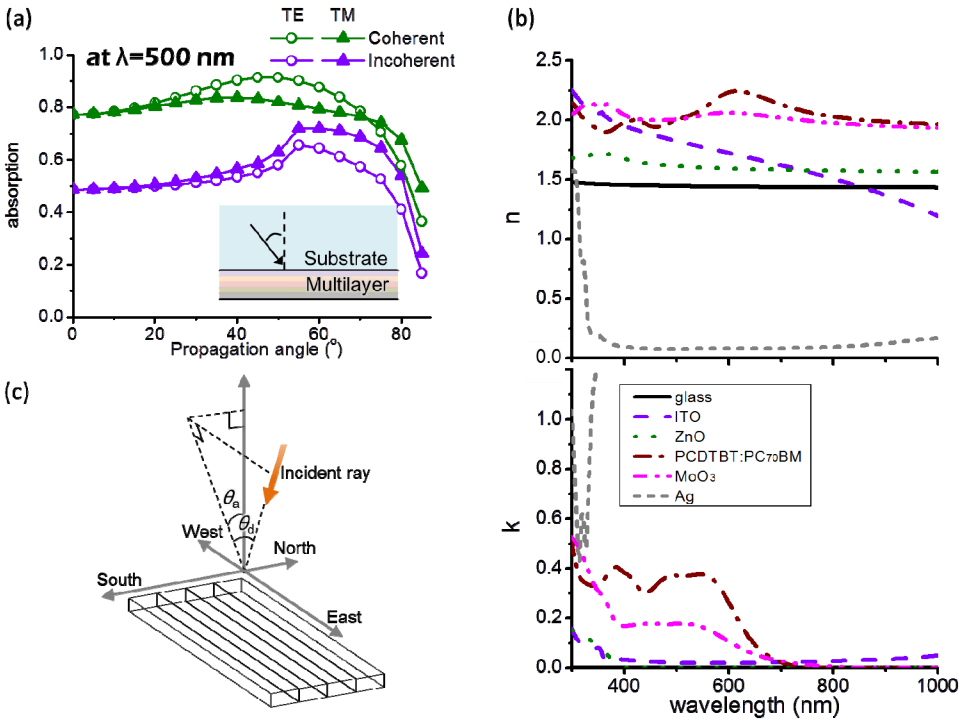

Fig. 1. (a) Absorption characteristics of the active layer according to the propagation angle variation (represented in the inset) for a thin-film PV using PCDTBT:$PC_{70}BM$ as an active material for TE (open) and TM (closed) polarized light with a wavelength of 500nm. The purple and green lines indicate the incoherent and coherent calculation, respectively. (b) n (real part) and k (imaginary part) values of the refractive indices used in the optical simulations. (c) Description of the annual (θ_a) and daily (θ_d) incident angle variation, where a 1D array structure is aligned along the east–west line.

oblique propagation with an incoherent optical calculation cannot represent the thin-film device characteristics [28, 29]. Figure 1(a) shows the absorption characteristics of the active layer along the propagation angle (θ_{prop}) calculated with and without considering the coherency of the incident light at a specific wavelength of 500 nm for a PV structure of glass / ITO (75 nm) / ZnO (27 nm) / PCDTBT:$PC_{70}BM$ (80 nm) / MoO_3 (10 nm) / Ag, where ITO, PCDTBT and $PC_{70}BM$ refer to indium tin oxide, poly[9'-hepta-decanyl-2,7-carbazole-alt-5,5-(4',7'-di-2-thienyl-2',1',3′-benzothiadiazole) and [6,6]-phenyl C 71 -butyric acid methyl ester, respectively [30–32]. The refractive indices for the simulations obtained by ellipsometry are shown in Fig. 1(b); they were assumed to be isotropic for simplification. Transfer-matrix formalism (TMF) for both TE and TM modes was used to calculate the absorption of the multilayer structure in the coherent model [28, 29]. In the incoherent model, Fresnel transmission and reflection were considered at each interface, as in the TMF calculation, but the coherencies between propagating waves were removed by considering the waves to be rays in the nano-scale multilayers. While the overall tendency of the absorption of both models agrees qualitatively, the incoherent model seriously underestimates the actual absorption as calculated by the coherent model, as revealed in Fig. 1(a). The discrepancy between the two models came from an interference effect that can exist only in the coherent region. The interference effect can induce extra absorption by concentrating the electromagnetic field in the active layers. This is the main difference between thin-film PVs and bulk PVs, in which the absorption increases only geometrically. Therefore, a proper optical simulation that considers such properties should be conducted to evaluate the performances of the ray-optical light trapping configurations on thin-film PVs. It should be

#182307 - $15.00 USD Received 21 Dec 2012; revised 7 Feb 2013; accepted 9 Feb 2013; published 21 Feb 2013
(C) 2013 OSA

noted that the sharp decrease of the active absorption in both models at a large propagation angle is mainly caused by the increased Fresnel reflections at the interface between the glass substrate and the top transparent electrode.

To date, many ray-optical light trapping schemes have been proposed to improve the light absorption of thin-film PVs through the creation of multiple bounces of the light on the active layer [23, 25–27]. For an analysis of a thin-film PV system with incoherent light trapping components, we implemented a hybrid type of custom-made simulation program written in MATLAB that combines geometrical ray tracing for incoherent regions and TMF for coherent regions. Since all the configurations considered in this report are one-dimensional arrays, only one unit structure with periodic boundary conditions is sufficient for the simulations. 200 incident rays were generated with equal spacing on top, and they were separated into the reflected rays and transmitted rays when they reach boundaries between different layers. The rays were tracked until their intensities become less than 10^{-6} of the initial intensity. The wavelength range of 300 ~ 1000 nm was considered to evaluate the performance of the PVs. In fact, the amount of absorption *enhancement* is dependent on the materials system and structures, contrary to the optical path length enhancement. Throughout this paper, the polymer PV structure using PCDTBT:$PC_{70}BM$ as an active material discussed in the previous section was used as a control device. PCDTBT:$PC_{70}BM$ polymer solar cells tend to show relatively high open circuit voltage (V_{oc}) and high IQE while their absorption efficiency is insufficient. The devices have light absorption efficiency of approximately 0.8 for the wavelength range of 400 ~ 650 nm [32]. PCDTBT:$PC_{70}BM$ was chosen because efficient light trapping can improve the PCE of the solar cells effectively. For estimation of the PCE of the PV device, we used values of V_{oc} = 0.88 V and fill factor (FF) = 0.61, which are typically obtained in our laboratory [31], and the internal quantum efficiency (IQE) was assumed to be 0.95 regardless of the wavelength, which was also taken from the literature [30]. These parameters are invariant regardless of the light trapping structures. Under the above conditions, an optical simulation shows that the reference PV cell has a PCE of 5.9% with a short circuit current (J_{sc}) of 11.0 mA/cm^2, which agrees well with the measured values [31].

For a complete evaluation of the given optical configurations, the entire annual movement of the sun must be taken into account because the performances of ray-optical light trapping schemes tend to be dependent on the incident angle of light. While the annual sun height variation is confined to within ± 23.5°, the daily sun movement covers the full 180° from east to west. The performance variation according to the daily sun movement may be minimized by aligning the cross-sectional plane of a 1D array type configuration perpendicular to the axis along east to west, as depicted in Fig. 1(c); the incident angle projected onto the cross-section is then constant for a complete day [23, 33–35]. In this paper, we define the annual incident angle (θ_a) as the incident angle projected onto the cross-section of a 1D array type configuration, which varies within ± 23.5° annually when the system is tilted at the altitude of the location. The daily incident angle (θ_d) is defined as the angle between the incident ray and the cross-section, which varies within ± 90° every day. Note that θ_a becomes 0° in spring and fall, and ± 23.5° in summer or winter, while θ_d of ± 90° corresponds to the time of sunrise or sunset.

3. Analysis on light trapping schemes

3.1 Micro lens array (MLA)

Trapping light using an MLA is an easy way to reduce the escape probability of internal rays and increase the probability that the rays will be absorbed by the photovoltaic cells. Tvingstedt et al. presented such a scheme using an MLA for light trapping with a highly restricted acceptance angle [23]. The configuration of a 1D MLA structure and corresponding simulation results are shown in Fig. 2(a) and 2(b), respectively. The incident rays are focused onto small entrances by the lens arrays, and blocking mirrors are implemented to prevent the internal rays from escaping the system. Assuming that the internal rays are sufficiently

#182307 - $15.00 USD Received 21 Dec 2012; revised 7 Feb 2013; accepted 9 Feb 2013; published 21 Feb 2013
(C) 2013 OSA

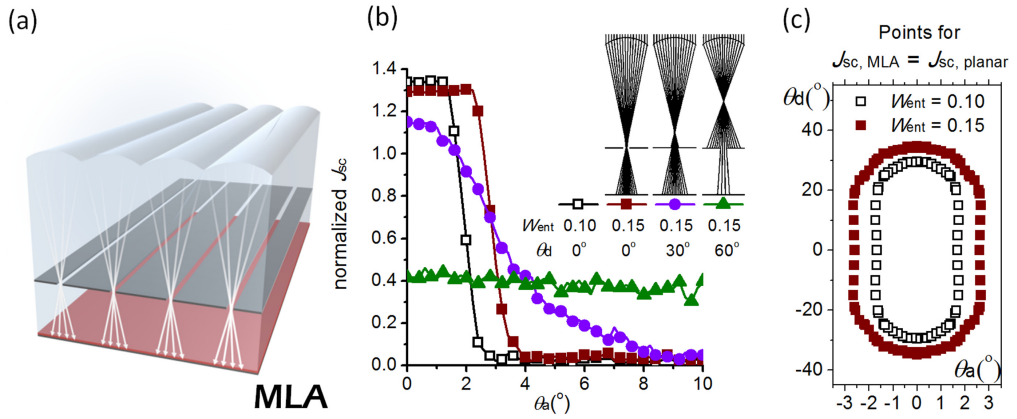

Fig. 2. (a) Light trapping system using MLA, (b) normalized J_{sc} variations with the variations of θ_a and θ_d for MLA-PV with different widths over the period (W_{ent}). Ray-traced cross-section images for $\theta_a = 0°$ are shown in the inset when $\theta_d = 0°$, 30° and 60°. To obtain a clear picture, the bottom cell and blocking mirrors were assumed to absorb the light for ray-tracing perfectly. (c) The contours of points (θ_a, θ_d), where the normalized J_{sc} becomes 1 for MLA-PVs when $W_{ent} = 0.10$ and 0.15, respectively.

randomized, the escape probability of the internal rays of this system is equal to the ratio of the entrance width to the period. For the simulation, the period of the structure was 400 μm and lens was designed by a cylindrical approximation with a radius of 328.9 μm; a cylindrical approximation was made considering the manufacturing process using isotropic etching in the literature [23, 36]. The theoretical focal length was 1000 μm for the structure with PMMA (n = 1.49). However, within the cylindrical approximation, the real curved surface of the vertex lens has larger curvature compared to the ideally thin lens shape and the practical focal length is shorter; therefore, we reduced the lens thickness to 940 μm.

Figure 2(b) shows the MLA-PV systems when $W_{ent} = 0.10$ and 0.15 at noon (i.e., $\theta_d = 0°$) resulting in the maximum J_{sc} enhancements of approx. 33.7% (PCE = 7.9%) and 29.3% (PCE = 7.6%), respectively, where W_{ent} indicates the relative entrance width over the period. However, no enhancement can be guaranteed when the annual acceptance angle is larger than 1.3° ($W_{ent} = 0.10$) and 2.2° ($W_{ent} = 0.15$); the enhancement is in a trade-off relationship with the value of W_{ent}, which eventually determines the acceptance angle. The W_{ent} value of the MLA-PV systems restricts the acceptance angle along not only θ_a but also θ_d. For example, when $\theta_d = 30°$ and 60°, the focal point became shorter; hence, the rays do not perfectly fall into the entrance even when $\theta_a = 0°$, as shown in the inset of Fig. 2(b). This occurs because the refraction on the lens surface cannot be dealt with by Snell's law independently for θ_a and θ_d. The points (θ_a, θ_d) of the normalized J_{sc} equal to 1 are plotted in Fig. 2(c). MLA-PV with a larger entrance ($W_{ent} = 0.15$) has a slightly larger acceptance angle region. Narrow acceptance angles of the MLA-PV systems in both directions imply that we need a 2D solar tracking system to make full use of the MLA, potentially increasing the cost of the PV system.

3.2 V-shaped structure

For bulk solar cells with a restricted acceptance angle of $2\theta < 180°$, it is known that the limit of the optical path length enhancement can be increased to $4n^2/\sin^2\theta$ [2, 21]. The fundamental trade-off relationship between the light trapping effect and the acceptance angle can explain the narrow acceptance angle of MLA-PV with a large J_{sc} enhancement. However, the trade-off relationship can be overcome using a larger PV area than the module area, such as in a V-shaped structure, as presented by Tvingstedt et al. and Rim et al., independently [25, 26].

#182307 - $15.00 USD Received 21 Dec 2012; revised 7 Feb 2013; accepted 9 Feb 2013; published 21 Feb 2013
(C) 2013 OSA

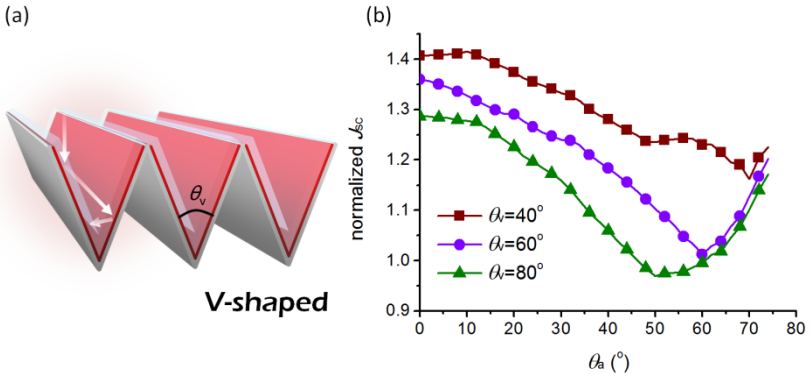

Fig. 3. (a) V-shaped light trapping configuration, (b) normalized J_{sc} variation with the variation of θ_a (where $\theta_d = 0°$) for V-shaped PVs with the different vertex angles (θ_v).

The V-shaped structure and its simulation results with various vertex angles (θ_v) are shown in Figs. 3(a) and 3(b), respectively. The J_{sc} enhancement increases with a decrease in θ_v and the maximum enhancement with a θ_v value of 40° is 40.7% (PCE = 8.3%), while it is still 35.7% with a θ_a value of 23.5°, which corresponds to the maximum incident angle for a whole year where the system is aligned at an east–west orientation and is tilted at the altitude of the location, as discussed above. Unlike the MLA system, the V-shaped configuration manipulates the incident light through reflection rather than refraction, implying that the ray trajectories that are projected on the cross-section of the V-shaped array are independent of θ_d and that the light trapping effect is mainly dependent on the value of θ_a. For an θ_a value larger than $(180° - \theta_v) / 2$, the V-shaped array does not trap the rays because all of the incident rays bounce on the PV only once and escape the system [26]. Hence, the normalized J_{sc} reaches its smallest point at θ_a values of 70°, 60° and 50° when θ_v is equal to 40°, 60° and 80°, respectively. It starts to increase again as θ_a increases given the reference J_{sc} of a planar PV with such an angle rapidly decreasing due to the increased optical loss caused by Fresnel reflection on the substrate.

As shown in Fig. 3(b), both a strong light trapping effect and a large acceptance angle are achieved simultaneously by the V-shaped scheme. Because the PV area over the module area increases as θ_v decreases (2.92-fold for $\theta_v = 40°$), the density of the light intensity is quite low over the PV area and the actual light trapping effect does not overcome the trade-off relationship with the acceptance angle in terms of the actual PV area. However, with the simple trick of folding planar PVs into a small module area, a greatly increased PCE is achieved over a large incident angle range. The cost of the increased material usage may not be a significant problem when using an inexpensive active material. Moreover, a tandem structure can be easily implemented using two different materials on each side, as proposed by Tvingstedt et al. [25]. This implies that we do not merely have to stack PVs with different band-gaps and that we can obtain both a multi-junction effect and an enhancement of the light trapping effect simultaneously. However, there remain some practical problems to be resolved, such as the complicated fabrication process, the increased volume, and the weights of the modules, with an unequal absorption distribution on each cell and an V_{oc} drop caused by the decreased absorption density [26].

3.3 Double parabolic trapper (DPT)

Lastly, in order to achieve perfect light absorption, we propose an ideal configuration, called DPT, as depicted in Fig. 4(a). It is well known that the parabola concentrates all of the normal incident rays to a focal point and that all of the rays passing the focal point in turn propagate parallel to the central axis upon the reflection on the parabola [see Fig. 4(a)]. We designed

#182307 - $15.00 USD Received 21 Dec 2012; revised 7 Feb 2013; accepted 9 Feb 2013; published 21 Feb 2013
(C) 2013 OSA

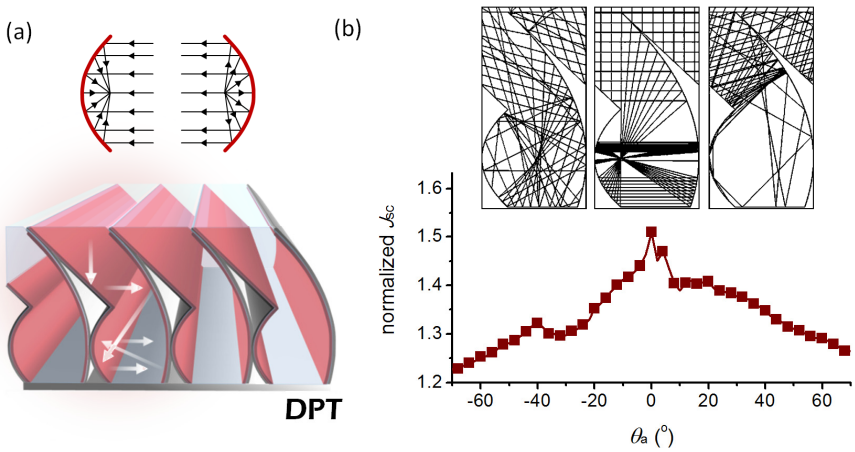

Fig. 4. (a) Geometrical characteristic of a parabola concentrating all of the incident rays parallel to the axis into a focus or reflecting them in a reverse manner (above), and DPT structure for perfect light trapping (below), (b) normalized J_{sc} variation with the variation of θ_a ($\theta_d = 0°$) for DPT-PV. Ray-traced images are also shown when $\theta_a = 0°$ and ± 23.5°, where only rays having power greater than 10% of an initial power appear.

two different sizes of parabolas which face each other, and which share the same focal point. Then, a ray once passing the point keeps circulating between the parabolas indefinitely.

If the PVs are implemented on the surface of the two parabolas and a front mirror, as shown in the red regions in Fig. 4(a), and if the multilayer structures do not disturb the direction of the reflected rays, perfect light trapping can be achieved. An enhancement of 50.9% was achieved when $\theta_a = 0°$ in the simulation, and the total device absorption becomes 100% in such a case. This implies that the PCE of the PV cell can be increased from 5.9% to 8.9% by light trapping only without any modification of the multilayer structure. Note that this does not imply that the external quantum efficiency (EQE) reaches the IQE, as the total device absorption also includes the parasitic absorption of the non-active layers, such as the metal electrode, which would not generate any photocurrent. The space between the two parabolas is assumed to be a glass mold in the simulations; it may be a practical consideration to evaporate PVs on the mold.

Interestingly, the DPT-PV scheme also shows good performance even for large variations of θ_a, although the tracing principle discussed above does not simply apply. Since the trapping scheme in DPT is also based on reflection, as in the V-shaped configuration, rather than refraction, the performance is almost independent of θ_d. Therefore, a J_{sc} enhancement of more than 30% is guaranteed for an entire year ($-23.5° < \theta_a < 23.5°$) in this system. The ray-traced results for $\theta_a = 0°$ and ± 23.5° are depicted in the insets of Fig. 4(b). Although the detailed working principle cannot easily be elucidated for each value of θ_a, the rays reflected by the tilted front PV bounce many times on other PV areas in various ways. The outstanding enhancement over a wide range of incident angles is due to the larger PV area compared to the module area (4.79-fold), as in the V-shaped system. The possibility of a tandem application implementing two different PVs on each parabolic side is also an advantage of DPT-PV, similar to the V-shaped configuration scheme discussed above. As in the V-shaped PV, unequal and low light intensity over the PV area of the DPT configurations may cause degradation of the electrical properties such as IQE, V_{oc}, and *FF*.

#182307 - $15.00 USD Received 21 Dec 2012; revised 7 Feb 2013; accepted 9 Feb 2013; published 21 Feb 2013
(C) 2013 OSA

Table 1. Summary of the light trapping characteristics for the MLA, V-shaped and DPT configurations

	MLA (Entrance 0.10)	V-shaped ($\theta_v = 40°$)	DPT
Enhancement (at $\theta_a = 0°$)	33.7%	40.7%	50.9%
Enhancement (at $\theta_a = 23.5°$)	≒ −100%	35.7%	38.9% (+ 23.5°) 32.1% (−23.5°)
PV area over module area	1	2.92	4.79
Tandem application	No	Yes	Yes
Fabrication process	Simple	Complicated	Complicated

4. Summary

In summary, we analyzed the light trapping effect of thin-film PVs by considering both ray-optical and wave-optical characteristics of the system. The trapping scheme using an MLA focuses on suppressing the escape of the internal rays and having them return to the photovoltaic layer. However, owing to a trade-off relationship, the performances of such schemes are highly restricted by the narrow acceptance angle. On the other hand, the V-shaped configuration utilizes a larger active area compared to the module area and hence further improves the light absorption without sacrificing the acceptance angle. Finally, we propose a configuration termed DPT as a perfect light trapping scheme. DPT-PV shows a J_{sc} enhancement of up to 50.9% when using the geometrical characteristics of a parabola at the normal incident angle while also showing a good angular response. In addition to the optical performance, the V-shaped and DPT schemes may also be used in tandem, but practical problems such as the complicated fabrication process should be overcome before commercialization can be realized. A comparison of the MLA, V-shaped and DPT schemes is summarized in Table 1.

Acknowledgments

We sincerely appreciate the financial support from the Basic Science Research Program through the National Research Foundation of Korea (NRF) funded by the Ministry of Education, Science and Technology (MEST) (2012-0003991). We also gratefully acknowledge support from the Center for Inorganic Photovoltaic Materials (2012–0001172) through a grant funded by the MEST, grant No. EEWS-2012-N01120012 from the EEWS Research Project of the office of the KAIST EEWS Initiative, KAIST Institute for the NanoCentury, and Samsung Display Co. C. Cho acknowledges financial support from the Korea Foundation for Advanced Studies (KFAS).

#182307 - $15.00 USD Received 21 Dec 2012; revised 7 Feb 2013; accepted 9 Feb 2013; published 21 Feb 2013
(C) 2013 OSA